

# Microfluidic volumetric flow determination using optical coherence tomography speckle: An autocorrelation approach

Lucas R. De Pretto,<sup>a)</sup> Gesse E. C. Nogueira, and Anderson Z. Freitas

*Instituto de Pesquisas Energéticas e Nucleares, IPEN–CNEN/SP, Avenida Lineu Prestes, 2242, 05508-000 São Paulo, Brazil*

(Received 18 December 2015; accepted 10 April 2016; published online 26 April 2016)

Functional modalities of Optical Coherence Tomography (OCT) based on speckle analysis are emerging in the literature. We propose a simple approach to the autocorrelation of OCT signal to enable volumetric flow rate differentiation, based on decorrelation time. Our results show that this technique could distinguish flows separated by  $3\ \mu\text{l}/\text{min}$ , limited by the acquisition speed of the system. We further perform a B-scan of gradient flow inside a microchannel, enabling the visualization of the drag effect on the walls. *Published by AIP Publishing.*

[<http://dx.doi.org/10.1063/1.4947282>]

## I. INTRODUCTION

Optical Coherence Tomography (OCT)<sup>1</sup> is a noninvasive, contactless imaging technique based on white-light interferometry that generates high resolution, cross-sectional images of scattering media. Such images provide morphological information about internal structures of samples. The micrometer-resolution, aligned with its penetration depth (in the order of a few millimeters, for biological samples<sup>2</sup>), places OCT in a unique spot among other imaging modalities, thus, OCT has found application in numerous fields of interest, notably in the biological researches.<sup>3–5</sup>

However, many studies demand not only morphological data regarding the sample. For that reason, it was not long until OCT adaptations that could provide additional information were reported on the literature.<sup>6</sup> Known as functional OCTs, those extensions enable further exploration of the subject under study that translates to more opportunities for clinical application. Among those extensions are the ones that aim to obtain information of flow or particle movement inside a sample. Of those, the most used is the Doppler OCT,<sup>7,8</sup> which measures the frequency shift in backscattered light caused by moving particles. Doppler OCT can, therefore, provide quantitative information regarding flow, including velocity and direction.<sup>9</sup> Since its report in the literature, it has been widely used in clinical studies. A serious limitation of technique, however, is its lack of sensitivity to flows perpendicular to the imaging beam, as no Doppler shift is detected. This represents a major drawback to numerous applications.

Other OCT approaches have been proposed to flow-detection functional imaging. Many of those are based on speckle noise. Speckle presents itself as a high contrast granular noise. If one were to imagine a rough surface illuminated by a coherent light source, reflections from different points of that surface can accumulate delays, originating interference patterns. In a distant observation point, the addition of these out-of-phase individual contributions results in

regions of constructive or destructive interference, forming the bright and dark spots of the speckle pattern.<sup>10</sup>

In OCT, despite the use of low coherence light sources, speckle arises as a consequence of the sensitivity to the phase of the cross correlation between the sample and reference optical fields.<sup>11</sup> However, in OCT, speckle is not limited only to the surface and, in fact, it is the pattern that arises from inside the sample that provides information about flows. The light travelling through the sample may accumulate phase delays due to multiple backscattering and forward scattering, altering the wavefront returning to the detector, and originating speckle patterns. Note, nevertheless, that the pattern is dependent on the individual scatterers causing the phase delays. Speckle, then, behaves differently through time, depending on such scatterers being static or moving. Different speckle analysis methods have been proposed to discern between the two scenarios using the speckle variance (SV) approach.<sup>12,13</sup>

Nonetheless, SV is a qualitative technique. Thus, recent studies proposed different models for the behavior of time-varying speckle in OCT, based on Dynamic Light Scattering (DLS) approach,<sup>14–17</sup> being able to obtain the decorrelation time in such a way as to semi-quantitatively determine flow velocity. Yet, those methods are time consuming and may not be viable in biological applications. Our work approaches the problem differently, by using a hybrid method through a straightforward analysis of the autocorrelation decay, giving enough information to evaluate changes in observed flow, based on the autocorrelation method proposed by Wang and Wang<sup>18</sup> with a new estimator associated with a DLS model, intending to obtain results in a manner that is both fast and robust.

## II. OBJECTIVES

In this work, we propose an approach to differentiate volumetric flow rate based on a simple observation parameter on the autocorrelation of OCT signal. We evaluate the method using controlled microflows and comparing the obtained results.

<sup>a)</sup>Author to whom correspondence should be addressed. Electronic mail: [lucas.de.pretto@usp.br](mailto:lucas.de.pretto@usp.br)

### III. MATERIALS AND METHODS

The data analysis method, the samples, and the OCT system used are described in the following.

#### A. Data analysis

The speckles originating from moving scatterers are expected to have larger fluctuations of intensity over time than the ones arising from static ones, due to the different phase contributions depending on the displacement of its source.<sup>14</sup> Owing to these intensity fluctuations, this "time-varying" pattern stays correlated for a shorter period of time when compared to the "static" one. Such occurrence has been exploited to map flow in OCT images in the past, but in a qualitative fashion.<sup>13,19</sup> Given this scenario, however, the autocorrelation function may pose as a viable way to discriminate between both situations—flow or static.

Hence, the proposed analysis consists in verifying and recording the intensity of speckle at a given fixed point in very short time intervals, in order for the intensity to still be correlated between sequential samples instead of being an independent sample (e.g., originating from a completely different scatterer distribution). Such intensities are obtained from A-scans and analyzed via autocorrelation through time.

After  $N$  A-scans are acquired consecutively in time for a given region, i.e., no beam scanning nor sample translation was performed during acquisition, a point  $p$  is selected and studied—i.e., a certain point in depth is fixed and this point is observed in all A-Scans acquired, enabling an analysis of its temporal behavior. The normalized autocorrelation  $R$  here used is

$$R(p, \tau) = \frac{\sum_{t=1}^{N-\tau} (I_{p,t\Delta} - \mu)(I_{p,t\Delta+\tau\Delta} - \mu)}{\sum_{t=1}^N (I_{p,t\Delta} - \mu)^2}, \quad (1)$$

with  $I_{p,t}$  being the intensity of the point  $p$  at given time  $t$ ;  $\tau$  is a lag interval; and  $\Delta$  is 1 divided by our sampling rate. For each point, its temporal average  $\mu$  is subtracted.

Calculating  $R$  for different lag intervals results in an array of the autocorrelation values of increasing lags and serves as a representative for the behavior of the speckle through time. At zero lag, the autocorrelation is expected to be total, resulting in a value of 1. However, as the time lag increases, those values should drop to zero, in which time the signal is no longer correlated to its delayed version (it "decorrelates"). The rate at which that decrease occurs is the parameter of interest for this analysis. This may be expressed as a simple observation parameter, such as the time it takes for the autocorrelation to decay to a certain value.

One may argue that the transit time of a scatterer through the volume of interest inside the sample directly impacts the intensity fluctuations observed, as it will affect the resulting phase delays. Ergo, the fluctuations might bear relation to the flow velocity. And, since the intensity fluctuations influence the "decorrelation" time, the autocorrelation values shall decrease at different rates depending on the flow velocity.

#### B. System setup

Since the fluctuations of intensity occur rapidly over time, a high acquisition rate was necessary in order to properly sample the signal. A custom OCT system was, then, built to achieve an adequate sampling rate. The light source used in the system is a frequency swept laser SL1325-P16 (Thorlabs, Newton, New Jersey, USA), with center wavelength of 1325 nm, tuning range of 120 nm, and repetition rate of 16 kHz, with a built-in Mach-Zehnder Interferometer (MZI). A Michelson type interferometer with balanced detection, INT-MSI-1300 (Thorlabs), suitable for wavelengths from 1250 to 1350 nm, was utilized. The output was coupled to an acquisition board NI PCI 5122 (National Instruments, Austin, Texas, USA). The system setup is illustrated in Fig. 1.

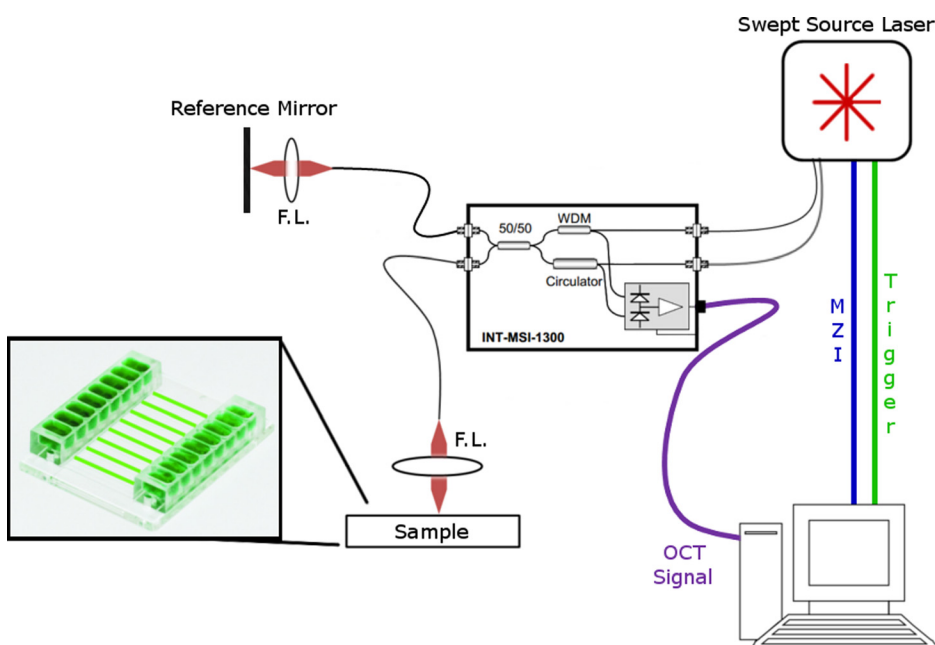


FIG. 1. OCT system setup illustration, with FL = focusing lens and WDM = wavelength-division multiplexer. The inset shows the microfluidic device used in the tests.

A custom software was developed in LabVIEW (National Instruments) programming environment, it communicates and controls the PCI 5122 acquisition board that handles three inputs, namely, the trigger for the laser source, the OCT signal, and a MZI signal, used for calibration.

The OCT interferometric signals are processed in A-scans only after all acquisitions are performed. There is no lateral scanning for the laser beam. In order to acquire data of different lateral locations, the sample was placed on a servo motor translator TDC001 (Thorlabs).

### C. Samples

For flow studies, a microfluidic device, Vena8 Fluoro+ (Cellix, Dublin, Leinster, Ireland), with 8 microchannels, each with a width of  $400\ \mu\text{m}$ , height of  $100\ \mu\text{m}$  and length of  $2.8\ \text{cm}$ , was used. To control the microflow on the Vena8 Fluoro+, the syringe pump ExiGo (Cellix) was utilized, with flow rate capability ranging from  $10\ \text{nL/min}$  up to  $20\ \text{ml/min}$ . Whole milk (3% fat) was used as the sample.

## IV. RESULTS AND DISCUSSION

With the aid of the syringe pump, the milk was subjected to different volumetric flow rates on the microchannel and sampled at the rate of  $8\ \text{kHz}$ . The microfluidic device was positioned so that the flow was perpendicular to the imaging beam. The autocorrelation values array for a single point at the center of the microchannel was calculated over 1024 consecutive acquisitions in time. Such a procedure was repeated five times and the arrays averaged. The resulting averaged array is plotted as a function of time lag.

In the first experiment, the milk was pumped at  $5\ \mu\text{l/min}$  through the microchannel, and the plot of the averaged array is shown in the Fig. 2(a).

It is important to note that the lag delays plotted go up to  $3.11 \times 10^{-2}\ \text{s}$ , which, with the acquisition rate used, corresponds to 250 A-scans. That owes to the fact that, once the values decay to zero, they remain oscillating around this value through all the remaining times, so, for better visualization, only the first 250 points are plotted. Apart from that, it is possible to note that the expected decrease in autocorrelation values with increasing delays is confirmed. Such results for the autocorrelation curve are not well documented in the OCT's speckle literature, being shown just for a few flow rates and techniques,<sup>16,18</sup> which makes it difficult for comparisons. Nevertheless, it is possible to note that the decrease happens monotonically in our result, contrary to the one reported in Ref. 18, which presents fluctuations along the decay. Also, according to the Gaussian model proposed by Ref. 17, zero-crossings are not expected to happen, and such occurrences, when present, may be due to variance in the estimates of  $R$  (caused by variance of  $\mu$  and  $R$  itself).

Noteworthy, as well, is the Power Spectral Density (PSD) of the signal, in the Fig. 2(b), demonstrating high contribution of frequencies below  $250\ \text{Hz}$  (3dB cutoff frequency) to the signal. As was the case for the autocorrelation curve, there are few examples of the PSD for speckle in OCT signal in the literature, with the work by Weiss *et al.*<sup>17</sup> being the only one known to these authors and, so, reports of

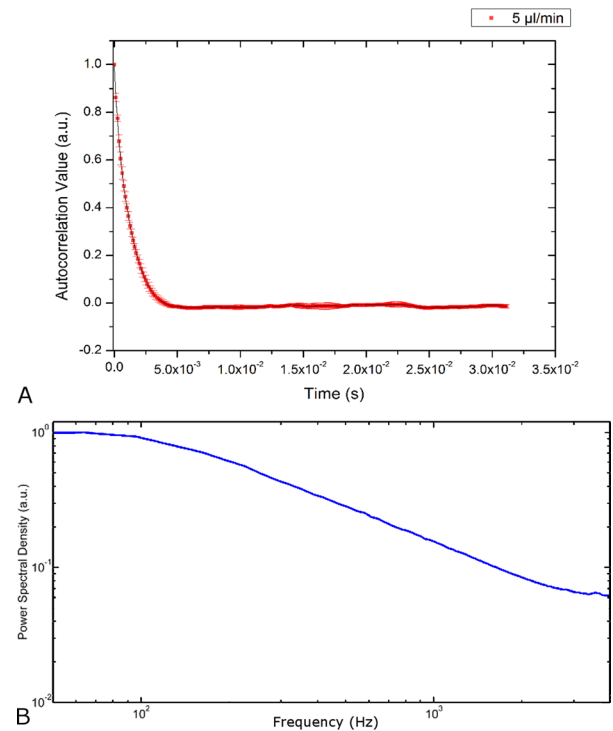


FIG. 2. Volumetric flow of  $5\ \mu\text{l/min}$ . (a) Autocorrelation array calculated. (b) Power spectrum of the OCT signal in log scale for the x and y axis. Error bars are presented as  $\pm$  standard deviation.

PSD for different approaches and systems are lacking. The spectrum agrees well with the one obtained by Weiss *et al.*<sup>17</sup> by using a curve fitting instead of a direct estimation as performed here.

Following the study, the milk was subjected to varying volumetric flow rates, namely, 1, 2, 3, 4, 5, 7, 10, and  $12\ \mu\text{l/min}$ . The procedure adopted to the first trial was repeated, averaging five autocorrelation arrays for each sample. Once again, only the first data points were plotted and, to enhance visualization, only four flows are displayed in the graph in Fig. 3. Complying with the expected outcome, the “decorrelation” does occur faster with higher flow rates. After long delays, all the curves overlap at values close to zero, as all the signals

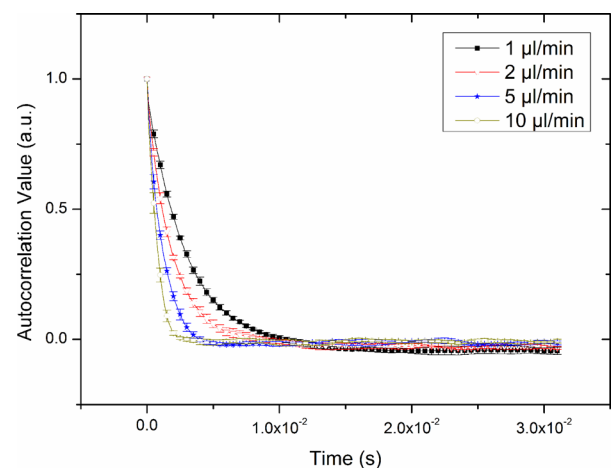


FIG. 3. Autocorrelation array for flows of  $1\ \mu\text{l/min}$ ,  $2\ \mu\text{l/min}$ ,  $5\ \mu\text{l/min}$ , and  $10\ \mu\text{l/min}$ . Error bars are presented as  $\pm$  standard deviation.

decorrelate. But the decrease occurs in a much steeper fashion for higher volumetric flows. It follows that the autocorrelation of speckle does bear relation with the velocity of the moving scatterers inside a sample.

We propose, therefore, a semi quantitative approach to differentiate the flow velocity, based on a simple analysis of the autocorrelation array, in order to be performed quickly. We established a “decorrelation time” as the time it takes for the autocorrelation values to drop below  $1/e$ . One can, thereby, plot this decorrelation time as a function of volumetric flow, graph shown in Fig. 4, and observe its behavior.

With that plot, it is now possible to note the clear trend of faster decorrelation for higher flow rates. Although being a simple point of observation in the whole array, the decorrelation time enables a method for comparison of results that is enough to differentiate flow rate change. To confirm that, one may observe that there is statistically significant differences in decorrelation time ( $p < 0.05$ , one-way ANOVA with Bonferroni and Bonholm as post-tests) for any pair of flow rates separated by, at least,  $3 \mu\text{l}/\text{min}$ . In Fig. 4 is also shown the Coefficient of Variation (CV) for each flow, ranging from 3.5% to 9.5%, comparable to the variability obtained by Weiss *et al.*,<sup>20</sup> but here using a direct estimation, as opposed to curve fitting, therefore obtaining similar results with a faster approach.

Although not reported in the speckle literature, to our knowledge, only the work of Wang and Wang<sup>18</sup> makes use of a simple analysis on the autocorrelation values of OCT to discriminate flow, however, using the slope of the curve, assuming a triangular autocorrelation function—a different approach than the one proposed here. A much more robust and recent model is the one present in Ref. 17, where contribution of transverse flow to the autocorrelation of OCT signal is Gaussian shaped, while the contribution of diffusive motion takes the form of an exponential decay. Hence, the slope, as an estimator, is not consistent with these more recent studies, as the autocorrelation would have no zero interceptions. Given this context, however, a simple method to differentiate flow velocity would be to estimate  $\sigma$ , the width of the Gaussian curve. The proposed estimator,  $1/e$ , is

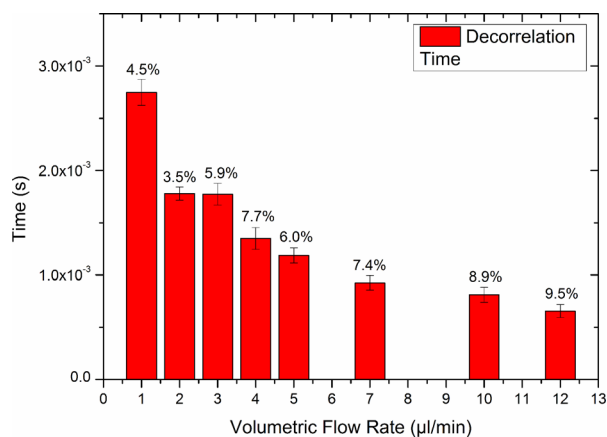


FIG. 4. Decorrelation time calculated for different flow rates. Note the trend of decrease with increasing volumetric flow. Error bars are presented as  $\pm$  standard deviation. Above each bar the coefficient of variation (in %) is reported.

proportional to  $\sqrt{2}\sigma$  and, therefore, proportional to flow velocity according to recent models.

Also, with the achieved resolution, as the decorrelation time gets smaller, it becomes increasingly difficult to be able to discern higher flows. This is due to the fact that the difference between calculated decorrelation times approaches the temporal resolution of the system, as illustrated by Fig. 5(a), with the results for the flows of  $30 \mu\text{l}/\text{min}$  and  $50 \mu\text{l}/\text{min}$  (the absence of error bars owes to the calculated results for the five arrays being the same, for both volumetric flows). Despite the gap between the flows, larger than any other previously studied, the difference between their decorrelation times equals to the temporal resolution— $1.25 \times 10^{-4}$  s—meaning that no other volumetric flow in the  $20 \mu\text{l}/\text{min}$  interval could be differentiated, without the use of interpolation. The power spectrum for the  $50 \mu\text{l}/\text{min}$ , in Fig. 5(b), may be observed to have a large broadening when compared to the  $5 \mu\text{l}/\text{min}$  one, discussed before, meaning that higher frequencies, up to 1.2 kHz (3 dB cutoff frequency), began to have greater contributions to the signal. Nevertheless, contributions of up to 4 kHz remain significant, meaning that the signal may have been undersampled by the system and, thus, no interpolation could take place. With all of the exposed, a higher acquisition rate may not only improve the sensitivity but also expand the range of flow rates that may be studied. In this study, the range at which the system better responded was up to  $12 \mu\text{l}/\text{min}$ .

In addition to those tests, to further demonstrate the applicability of the method, the microchannel was placed on an automated translator and laterally displaced, with five series of acquisitions taken for each lateral location. After completed the sampling at a given point, the sample was laterally translated  $25 \mu\text{m}$ , and new acquisitions were made. This procedure was repeated 15 times, with the first iteration performed at  $5 \mu\text{m}$  away from the left wall inside the sample, to verify the influence of the proximity to the wall on the

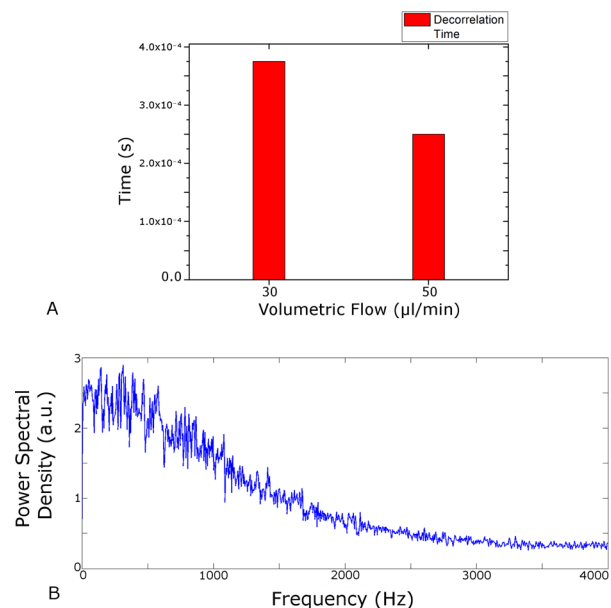


FIG. 5. (a) Decorrelation time calculated for volumetric flows of  $30 \mu\text{l}/\text{min}$  and  $50 \mu\text{l}/\text{min}$ . (b) Power spectrum of OCT signal for the flow of  $50 \mu\text{l}/\text{min}$ .

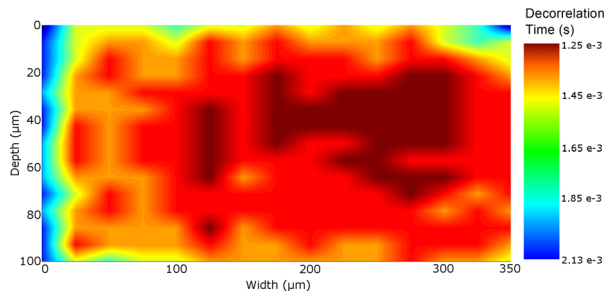


FIG. 6. Decorrelation time calculated for several points inside the microchannel while milk is pumped at  $5 \mu\text{l}/\text{min}$ . It functions as a B-scan of flow gradient inside the microchannel.

flow. The height of the microchannel corresponded to 15 points of the A-scan (axial resolution of approximately  $6.6 \mu\text{m}$ ). For each of the resulting 225 points, the decorrelation time was computed. The flow of milk was kept constant at  $5 \mu\text{l}/\text{min}$ . A spline interpolation was performed on those results, to enhance quality, and converted to a false-color image shown in Fig. 6.

This is, therefore, a B-scan of flow rates. It enables the visualization of flow rate changes inside the microchannel as well as the uniformity of the flow throughout the microfluidic circuit and is a practical application of the proposed approach. It is possible to see how the higher flow occurs at the center of the microchannel, expressed by reddish colors (meaning lower decorrelation time in the scale shown), as opposed to the flow near the walls, which are lower (bluish colors). This is expected since the drag exerted on the fluid by the walls affects the flow. It is specially perceptible at the leftmost column on the image, which is the acquisition  $5 \mu\text{m}$  away from the wall and, consequently, it is more affected by the drag. The opposite wall is not observable, as it was not measured in this experiment. The decorrelation times of the region with higher flow are in good agreement with those previously calculated for  $5 \mu\text{l}/\text{min}$ . This test highlights the usability of the analysis and gives a result otherwise reported in the literature only through techniques based on fitting models. So, we could achieve the same type of result faster and with less computational power.

## V. CONCLUSIONS

Through the speckle in OCT, it is possible to obtain information regarding the sample, going beyond morphological information. In the present work, we have shown that a simple approach to the autocorrelation analysis is enough to exploit this useful information in a semi-quantitative manner.

We demonstrated that through a parameter of observation in the autocorrelation array of increasing lags, it was possible to discern the different volumetric flows at which a sample was pumped inside a microchannel. The results were consistent, and, with the setup used, differences as low as

$3 \mu\text{l}/\text{min}$  were perceived with statistical significance. Even the different flow rates inside the microchannel could be distinguished through the use of our approach, which provides the ability to perform B-scans of flow velocities. Despite not being able to fully quantify the flow sampled, as other approaches using autocorrelation, the proposed method is relevant for its simplicity and fast computation while still providing discrimination of flow with good sensitivity, finding application in studies interested in observing changes in the flow rate in biological or simulated scenarios.

With all of that, the approach was demonstrated to have good results for the expected behavior and is a viable tool to be applied with OCT, requiring no modification of system setup nor prior sample preparation.

## ACKNOWLEDGMENTS

The authors thank Marcus Paulo Raelle for the discussions and useful insights provided. This study was supported by São Paulo Research Foundation-FAPESP (Grant Nos. 2013/05492-9 and 2013/09311-9) and The National Council for Scientific and Technological Development (CNPq), Brazil (Grant Nos. 449440/2014-1 and 309367/2013-1).

- <sup>1</sup>D. Huang, E. A. Swanson, C. P. Lin, J. S. Schuman, W. G. Stinson, W. Chang, M. R. Hee, T. Flotte, K. Gregory, C. A. Puliafito, and J. G. Fujimoto, *Science* **254**, 1178 (1991).
- <sup>2</sup>V. M. Kodach, J. Kalkman, D. J. Faber, and T. G. van Leeuwen, *Biomed. Opt. Express* **1**, 176 (2010).
- <sup>3</sup>W. Drexler and J. G. Fujimoto, *Optical Coherence Tomography: Technology and Applications* (Springer, 2008).
- <sup>4</sup>E. Sattler, R. Kästle, and J. Welzel, *J. Biomed. Opt.* **18**, 061224 (2013).
- <sup>5</sup>A. M. Zysk, F. T. Nguyen, A. L. Oldenburg, D. L. Marks, and S. A. Boppart, *J. Biomed. Opt.* **12**, 051403 (2007).
- <sup>6</sup>J. Kim, W. Brown, J. R. Maher, H. Levinson, and A. Wax, *Phys. Med. Biol.* **60**, R211 (2015).
- <sup>7</sup>S. Yazdanfar, M. Kulkarni, and J. Izatt, *Opt. Express* **1**, 424 (1997).
- <sup>8</sup>X. J. Wang, T. E. Milner, and J. S. Nelson, *Opt. Lett.* **20**, 1337 (1995).
- <sup>9</sup>R. A. Leitgeb, R. M. Werkmeister, C. Blatter, and L. Schmetterer, *Prog. Retin. Eye Res.* **41**, 26 (2014).
- <sup>10</sup>J. W. Goodman, *J. Opt. Soc. Am.* **66**, 1145 (1976).
- <sup>11</sup>J. M. Schmitt, S. H. Xiang, and K. M. Yung, *J. Biomed. Opt.* **4**, 95 (1999).
- <sup>12</sup>X. Liu, K. Zhang, Y. Huang, and J. U. Kang, *Biomed. Opt. Express* **2**, 2995 (2011).
- <sup>13</sup>A. Mariampillai, B. A. Standish, E. H. Moriyama, M. Khurana, N. R. Munce, M. K. K. Leung, J. Jiang, A. Cable, B. C. Wilson, I. A. Vitkin, and V. X. D. Yang, *Opt. Lett.* **33**, 1530 (2008).
- <sup>14</sup>J. Lee, W. Wu, J. Y. Jiang, B. Zhu, and D. A. Boas, *Opt. Express* **20**, 22262 (2012).
- <sup>15</sup>X. Liu, Y. Huang, J. C. Ramella-Roman, S. A. Mathews, and J. U. Kang, *Opt. Lett.* **38**, 805 (2013).
- <sup>16</sup>N. Uribe-Patarroyo, M. Villiger, and B. E. Bouma, *Opt. Express* **22**, 24411 (2014).
- <sup>17</sup>N. Weiss, T. G. v. Leeuwen, and J. Kalkman, *Phys Rev E* **88**, 042312-1 (2013).
- <sup>18</sup>Y. Wang and R. Wang, *Opt. Lett.* **35**, 3538 (2010).
- <sup>19</sup>A. Mariampillai, M. K. K. Leung, M. Jarvi, B. A. Standish, K. Lee, B. C. Wilson, A. Vitkin, and V. X. D. Yang, *Opt. Lett.* **35**, 1257 (2010).
- <sup>20</sup>N. Weiss, T. G. v. Leeuwen, and J. Kalkman, *Opt. Express* **23**, 3448 (2015).